Deblending a sparse OBN survey acquired with a generalized survey optimization scheme

Matthew Salgadoe, Bartosz Szydlik, Azat Kuliev and Christopher McMorland (SLB)*

Summary

We present the results of deblending a sparse ocean-bottom node survey located in Green Canyon, in the US Gulf of Mexico. The survey was designed using a constrained optimization scheme (Kumar et al., 2023) which resulted in optimized source locations in time and space. We show that these newly acquired data exhibit more randomization of interfering energy and this can prevent strong interference energy from contaminating weak signal. The high degree of randomization leads to improved deblending results when using an iterative multistage source separation process when compared with a conventional flip-flop-flap simultaneous source shooting scheme. This ultimately leads to better removal of interference noise. The combination of improved shooting geometry and source separation flow provides deblended data that shows uplift to subsalt structures even when imaged with an initial earth model.

Introduction

In the past few years there has been an increased effort in acquiring sparse ocean-bottom node (OBN) surveys in the northern Gulf of Mexico. Following recent successes, many sparse OBN surveys are in progress or planned. These surveys are large in scale, covering several thousand square kilometers of node coverage, with an even larger source effort.

Lately a number of these surveys have been concentrated in the Green Canyon protraction area in the US Gulf of Mexico. Due to complex salt geometries and associated illumination requirements, this area has proved challenging in terms of seismic imaging despite the large amount of legacy data available and continuous reprocessing of these towed streamer datasets with the latest processing technologies. The key to improved imaging lies in reducing the uncertainty in the definition of salt canopies and welds in the area.

Large scale OBN surveys have been proven to provide an uplift in imaging in complex geological areas, where salt regimes provide difficulty in characterizing and identifying exploration targets. This uplift comes from two sources. Firstly, the OBN data are full azimuth, which helps to improve illumination of subsalt exploration targets. Secondly, the OBN data are ideally suited for full-waveform inversion (FWI) with extremely large offsets that reach 60 km, to capture diving waves down to Louann Salt. Enhanced template matching FWI (ETM-FWI) driven earth model updates are better constrained and stabilized by utilizing the long-offset OBN data, combined with an increase in illumination in subsalt areas (Vigh et al., 2021). Reducing the uncertainty in the updated earth model provides better imaging of both legacy streamer datasets and the OBN data, ultimately leading to a better understanding of exploration and development targets.

Large-scale sparse OBN surveys need to be acquired in simultaneous source mode to be cost-effective and to overcome time constraints imposed by nodal acquisition limitations.

Data acquisition

The OBN survey in question covers an area of approximately 3500 km^2 with nodes deployed on the seafloor in a 1200 m x 1200 m grid, resulting in over 2400 nodes to be subsequently processed. The seabed in the survey area varies rapidly from ~85 m to ~2200 m. The source effort involved two source vessels acquiring 1.9 million shots on a nominal 50-m inline by 100-m crossline grid over an area of 8554 km^2. The source carpet extended from 15 to 18 km past the edge of the node carpet. This leads to a nominal maximum offset of around 30 km, but up to 60 km is not uncommon.

The need for simultaneous-source shooting as a means of reducing acquisition cost must be balanced against two further challenges. Firstly, the simultaneous-source shooting scheme must be designed such that interfering source energy is sufficiently randomized to aid its successful removal. Secondly, for this seismic data to be usable and achieve the survey aims, a robust deblending scheme must be in place, with particular care taken to ensure low frequencies are suitably preserved for FWI.

Kumar et al., 2023 presented a methodology for designing an optimal survey acquisition scheme, using spectral-gap-based rank minimization to generate the design geometry with random time dithers. This method is known as generalized survey optimization with constraints (GSOC). GSOC involves solving this optimization problem, which generates a more randomized acquisition geometry for both source and node locations in both horizontal directions. Sampling constraints can also be introduced, such as random spatial dithers in the inline and crossline sense, or user defined spatial constraints, such as requiring that two sources adjacent along a source line or along a crossline do not fall within a certain spatial distance of each other.

Additionally, both environmental and instrumental constraints can be incorporated. For example, the limitations of hardware and software associated with the in-sea source equipment and onboard source controllers can necessitate that successive sources should not fire within a certain time window to allow the air gun compressors suitable time to refill, or to allow appropriate time for the shot controller to process the next shot information.

The optimization scheme resulted in the following updates to the source geometry. Nominally, the source carpet uses a 50-m inline and 100-m crossline spacing. This was achieved using one vessel that towed three source arrays, each separated by 100 m, resulting in the acquisition of three source lines during one sail-line pass. It is not currently possible to apply spatial dithering to the crossline separation of the three arrays for a single vessel, however it can be applied to sail line separation. This was nominally 300 m, but using the GSOC methodology the sail line separation would vary by ±15 m.

Figure 1 shows the sail line separation as a function of sail line in blue for the GSOC survey. Also included in red, for comparison, are the sail line separations for a nearby sparse OBN survey acquired using a conventional, flip-flop-flap acquisition design scheme. The comparison survey had a consistent 300 m separation with small deviations due to infrastructure or currents. The blue GSOC points show the randomized nature of the crossline spacing and the effect of the spatial dither.

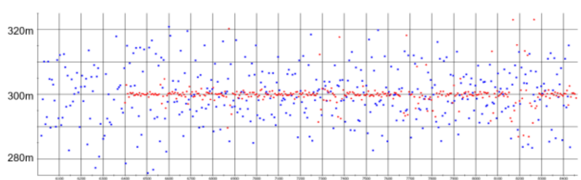

Figure 1 Sail line separation for each sail line in the GSOC survey (blue) and flip-flop-flap survey (red)

A higher level of randomization can be achieved in the inline sense than the crossline, as this can be more easily controlled with random time dithers, boat speed, and spatial dithering. Figure 2 (b) is a histogram representation of the shot-to-shot distance in the inline direction for this GSOC survey; note the spread of values from 30 to 60 m. The flip-flop-flap simultaneous source survey is also shown for comparison in red in Figure 2 (a). In this histogram, there is a clear peak around 50 m, which is the nominal shot spacing, and the spread is much smaller than the GSOC survey.

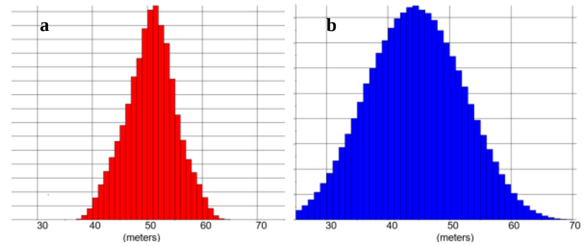

Figure 2 Shot-to-shot distance for flip-flop-flap survey (a) and GSOC survey (b)

A final component of the inline shooting scheme is the random time dither shown in Figure 3. Larger dithers, from -3 to 6 seconds were utilized in the GSOC survey (b) to achieve a higher level of randomization. This contrasts with the 1-second maximum dither values in the conventional flip-flop-flap survey (a).

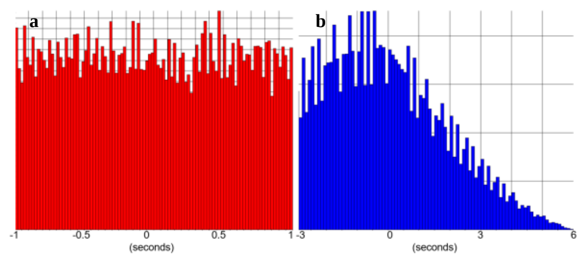

Figure 3 Shot dither values used in the two shooting schemes, (a) shows flip-flop-flap and (b) shows GSOC shooting.

Simultaneous-source deblending

For this data, we used the multistage source-separation process described by Amin et al. (2021).

First, we transformed the common node gathers to a sparsity promoting domain, and then used prior information (in this case, moveout) and coherency filters to create an initial estimate of the signal. This signal model can then be transformed to a model of the blended source energy by using information on shot timing and locations. The estimated signal and blended noise model are then subtracted from the input data to give a residual estimate. This residual is combined with the signal model, and then moves on to the next iteration of deblending, whereby the above process of estimating updated signal and noise models continues.

The thresholding criteria used for the coherency filtering can be lessened for each successive iteration of signal estimation and noise model building. The level of residual is monitored throughout the process, and the process can be stopped when the residual level is small relative to the signal estimate and blended shot model.

Figure 4 (a) shows a typical hydrophone gather from this survey resulting from our new acquisition scheme. Figure 4

(b) shows the same common node gather after several iterations of the multistage deblending process. The high amplitude energy associated with the interfering sources has been removed, especially in the zoomed highlighted areas (c & d), where weak primary signal and early arrivals have been uncovered.

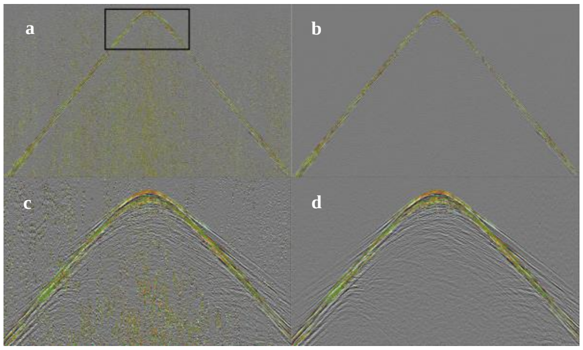

Figure 4 Hydrophone gather before (a) and after (b) deblending. Zoom of shallow reflections before (c) and after (d)

When these newly acquired data are imaged, the higher degree of randomness with respect to the blended energy becomes more apparent. Figure 5 shows a 12-Hz RTM of the hydrophone downgoing component, using an initial earth model before any FWI-driven earth model updates.

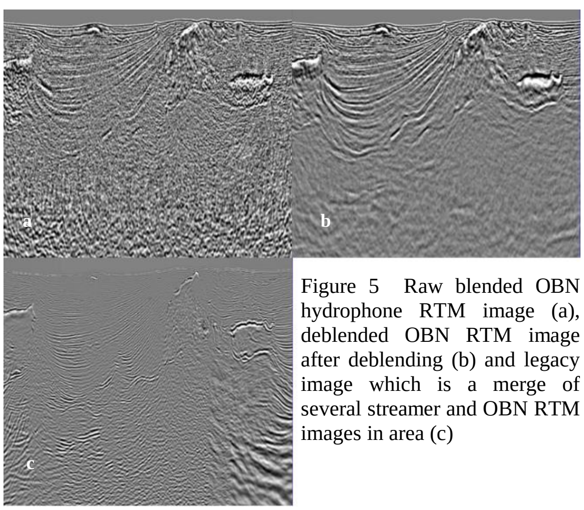

Figure 5 Raw blended OBN hydrophone RTM image (a), deblended OBN RTM image after deblending (b) and legacy image which is a merge of several streamer and OBN RTM images in area (c)

Even before deblending (a) shallow aspects of the sub-surface are identifiable but deeper events are still masked by the blended energy. After deblending (b), we see the uplift in the image, with the removal of the high amplitude energy associated with the blended source energy. Importantly the raw nodal data, when imaged (a), already show uplift against the legacy products available in the area (c).

The primary aim of this survey was to provide full-azimuth, long-offset OBN data for use in FWI and improve illumination of complex structures and deep events. A key QC used during FWI is the phase ring plot. To create the plot, the instantaneous phase is extracted for a specific frequency in a window, then plotted for every shot for each node gather. Examples of the phase ring are shown in Figure 6 before (a) and after (b) deblending, respectively. At 1.8 Hz, we see that the raw blended data have good coherency even at low frequencies, showing the blended energy exhibits the high degrees of randomness expected from this survey design scheme. After deblending we see uplift to the phase ring QC, where coherency has increased, and the interference noise is removed.

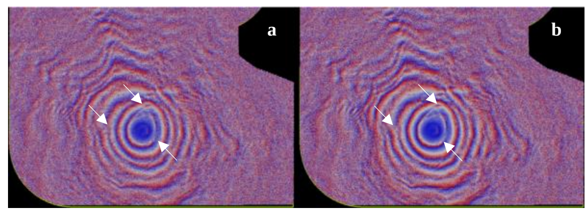

Figure 6 Single node phase ring plot at 1.8 Hz before (a) and after (b) deblending. Stripes associated with interfering source energy are highlighted, showing reduction and improved coherency in (b).

Discussion

With the Green Canyon area being an extremely prospective area for exploration and development targets, several sparse OBN surveys have been acquired in recent years. For reasons mentioned previously these were acquired in simultaneous source mode and have the same underlying geometry on both the node and source side. Salgadoe et al., 2022, have previously shown successful deblending of sparse OBN data shot in flip-flop-flap simultaneous source mode in the Green Canyon area. This provides an opportunity to compare the seismic data acquired using the optimized acquisition scheme with data acquired on a more conventional periodic time grid with random time dithers.

The conventional simultaneous source survey we compare with had nodes spaced every 1200 m x 1200 m. The source carpet was a 50-m inline by 100-m crossline grid. Figure 1 showed source lines were spaced every 100 m, with very little variation from the 300 m vessel sail line separation. For the inline direction, the sources were approximately fired every 50 m, with a small deviation from this. The sources were fired in a flip-flop-flap cycle, with a shot fired every 16.66 m from a single vessel.

Figure 7 shows the comparison of shot-to-shot time for each of these two surveys. We see the spread in the shot timing in the GSOC survey in Figure 7(b), with the range from 3 to 12 seconds. The minimum 3-second shot time interval was imposed due to hardware constraints on the source vessels.

This contrasts with the flip-flop-flap survey in Figure 7 (a). Here we see the nominal shot-to-shot time of 7 seconds clearly in the histogram, with much less spread about that this nominal time.

A representative nodal gather is also shown alongside the shot time histogram. It can clearly be seen that the flip-flop-flap survey results in randomized bands of interference energy approximately every 7 seconds. We can compare this with the GSOC data, where this banding of interference energy is less noticeable, due to the more varied shot-to-shot time, as seen in the histogram.

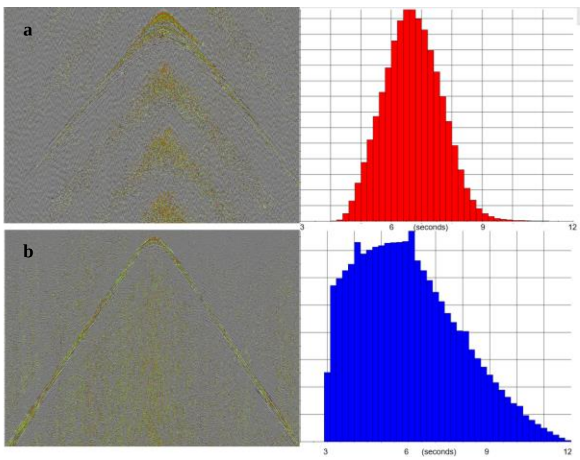

Figure 7 Hydrophone blended gather and shot-to-shot time comparison between flip-flop-flap (a) and GSOC acquisition (b)

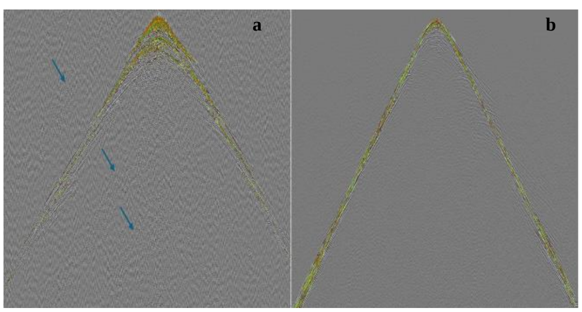

Figure 8 Hydrophone data after deblending for same gathers shown in figure 7 for flip-flop-flap (a), and GSOC shooting (b). Note in (a) the low level of residual interference energy present in highlighted areas.

Kumar et al., 2021 described the strong-on-weak phenomenon and some of its key characteristics, which are evident in the flip-flop-flap example in Figure 7 (a). These include how self-interference from the same vessel's shots appear in compressed hyperbolic bands every 7 seconds and then how self-interference from the same shot repeats in bands approximately every 21 seconds. Utilizing the separation process can overcome most of these issues, and remove these strong bands of interference. However, there is still some low-level residual interference energy left in these bands as highlighted in Figure 8 (a). In contrast, Figure 8 (b), again, shows the GSOC deblend result, and this type of residual energy is not apparent.

Conclusions

We have detailed the large-scale implementation of a rank minimization technique to generate acquisition design for simultaneous source surveys.

The blended noise from interfering sources is more randomized in nature when shot using this scheme, and this is beneficial for data acquired in the survey area where large shallow salt bodies are present. This randomization allows the blended noise to be more evenly distributed, helping to separate it from signal in a sparsity- promoting domain.

The combination of the survey design scheme and the deblending workflow yields OBN data that provides full-azimuth, long-offset data with early arrivals and refractions intact, which is invaluable for constraining FWI model updates. Additionally, the cleaner OBN data even when imaged with an immature model, provides an improved understanding of the complex sub-salt structures in the area when compared with available legacy data.

The results of acquiring data with this scheme leads to a more efficient shooting schedule, and results in acquired data that has lower levels of residual blended energy than previous acquisition schemes, which leads to uplift in final images over the area.

Acknowledgements

The authors thank SLB Multiclient and TGS for permission to use the data shown in this presentation.